

Variation of reflectivity and colour in SnO₂/Ag/SnO₂ structure with Nb₂O₅ and SiO₂ index matching layer

Jin-Gyun Kim and Gun-Eik Jang*

Department of Materials Engineering, Chungbuk National University, Cheongju 362-763, Korea

The reflectivity and colour variation in SnO₂/Ag/SnO₂/SiO₂/Nb₂O₅ multi layer films on glass substrate were investigated with respect to the top layer SnO₂ thickness and IM (Index matching layer) layer. Initially SnO₂/Ag/SnO₂/SiO₂/Nb₂O₅ multi layer films on glass substrate were deposited at room temperature by RF/DC magnetron sputtering method. EMP simulation results suggested that the multilayered thin film of SnO₂ (40 nm)/Ag (10 nm)/SnO₂ (30 nm)/SiO₂ (10 nm)/Nb₂O₅ (10 nm) exhibited the highest visible transmittance of 90.1% at 550 nm, whereas experimentally measured transmittance showed 85.1%, somewhat lower than simulation data. Reflectivities of SnO₂ (40 nm)/Ag (10 nm)/SnO₂ (30 nm)/SiO₂ (10 nm)/Nb₂O₅ (10 nm) multi layer film at 450 nm and 550 nm of visible range, were 10.4% and 10.6% measured on the top of multi-layer film stackup, respectively. However, reflectivities with IM layer only were 10.8% and 12.4%, suggesting that reflectivity variation was approximately within 2%. From the L*a*b* colour space represented by reflectivity spectra, it was found that the lightness (+ L*) decreased from 91.2 to 89.4, whereas the yellowness (+ b*) increased from 0.77 to 1.47, with increasing SnO₂ top layer thickness in multi-layer film.

Key words: TMT structure, Reflectivity, Index matching layer, L*a*b* colour space.

Introduction

In recent years, many researchers are dedicated to investigate the visible transmittance and electrical resistivity of Transparent conducting oxides (TCO) films for a wide variety of applications in optoelectronic, solar cell, organic light emitting diodes, and liquid crystal displays [1, 2]. Among many TCO materials [3-8], SnO₂ is currently being extensively studied as one of potential candidates to substitute the widely used Indium Tin Oxide (ITO), due to its thermal stability under hydrogen plasma processes and chemical stability in both acid and alkaline medium [9, 10].

Recently, TCO/metal/TCO (TMT) multi layer structures have been designed to achieve both high conductivity and high transmittance in the visible range and also showed relatively better chemical stability than single-layered film [11-17].

In commercial application using TCO material, touch screens are becoming increasingly popular because of their ease and versatility of operation as well as their cost effectiveness. However, when the touch sensor panel in touch screens composed with TCO and adhesive is used in a bright environment, incident light can hit the interfaces between those layers of the stackup having mismatched refractive indices and can reflect off those interfaces. The light reflected from

those interfaces can give rise to the appearance of fringes on the touch sensor panel, which can be visually distracting.

In order to reduce the fringe effect, reflectance change at the interface, by placing the index matching (IM) layer with high and low refractive indices under TCO material, could be one of possible solutions in TMT structure. It was already known that the presence of IM layer can reduce the amount of reflection at the adhesive - ITO interface, which in turn, can reduce the interference of reflected light and the appearance of fringes on the touch sensor panel [18, 19]. However, not many previous works have been undertaken in the modification of optical characteristics through the addition of IM layer with high and low refractive indices into tri-layer structure.

In this work, a hybrid structure of SnO₂/Ag/SnO₂ film with IM layer has been designed. SiO₂ ($n = 1.46$) and Nb₂O₅ ($n = 2.34$) with low and high refractive indices, which have been the most successful application in electronic industry as electrical contact, were selected as IM materials. The aim of present work is to evaluate the optical spectra and colour variation of SnO₂/Ag/SnO₂/SiO₂/Nb₂O₅ multilayer film with different top layer thickness of SnO₂ and the effect of IM layer on reflectivity in SnO₂/Ag/SnO₂ film.

Experimental

Simulation

Prior to the experiments, one of the optical programs

*Corresponding author:
Tel : +82-43-261-2412
Fax: +82-43-271-3222
E-mail: gejang@chungbuk.ac.kr

named Essential Macleod Program (EMP) was used to simulate the optical characteristics such as transmittance, reflectance and color in the multi layer thin films. The EMP was processed through the following steps; first, construction parameters such as reflectance and extinction coefficient of SnO_2 , Ag, SiO_2 and Nb_2O_5 , respectively, which were calculated by ellipsometry measurement, were input in the program. Second, $\text{SnO}_2/\text{Ag}/\text{SnO}_2/\text{SiO}_2/\text{Nb}_2\text{O}_5$ multi layers were designed and simulated with various parameters such as wavelength ranges (380-780 nm), thickness (10-55 nm) of and layers of structure. Finally, analysis on the parameter effect was performed with system modification for optical properties whether it is appropriated for the optimum simulation.

Film preparation

For the purpose of study, SnO_2 (40-55 nm)/Ag (10 nm)/ SnO_2 (30 nm)/ SiO_2 (10 nm)/ Nb_2O_5 (10 nm) multi layer film with more than about 85% transmittance was selected after taking a number of simulation by modifying the stacking sequence and adjusting the thickness of each layer. A hybrid structure of $\text{SnO}_2/\text{Ag}/\text{SnO}_2/\text{SiO}_2/\text{Nb}_2\text{O}_5$ was deposited on soda lime glass substrates by sequential RF/DC magnetron sputtering at room temperature. In order to compare the optical characteristic of $\text{SnO}_2/\text{Ag}/\text{SnO}_2/\text{SiO}_2/\text{Nb}_2\text{O}_5$ film, $\text{SnO}_2/\text{Ag}/\text{SnO}_2$ film was prepared as a reference. Fig. 1 shows a schematic diagram illustrating the structure of $\text{SnO}_2/\text{Ag}/\text{SnO}_2/\text{SiO}_2/\text{Nb}_2\text{O}_5$ multi layer film. Prior to deposition, soda-lime glass ($75 \times 25 \times 1 \text{ mm}^3$) was ultrasonically cleaned in acetone, ethanol and IPA for 30 min at 50°C . Thin film layers of SnO_2 , SiO_2 , and Nb_2O_5 were deposited by RF magnetron sputtering onto soda-lime glass substrates at room temperature. High purity Ar (35 sccm) was introduced into the chamber by mass flow meter with the total pressure maintained at 5.5 mTorr. Ag layer was deposited by DC magnetron sputtering. The total film

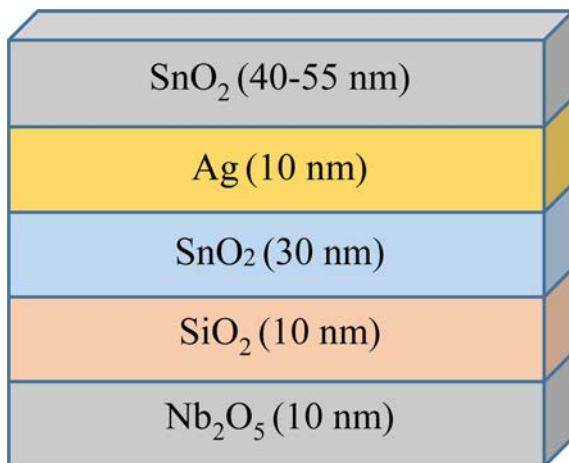


Fig. 1. A schematic diagram illustrating the structure of $\text{SnO}_2/\text{Ag}/\text{SnO}_2/\text{SiO}_2/\text{Nb}_2\text{O}_5$ multi layer film.

thickness was about 100 nm. The thickness of each layer was controlled by increase in the sputtering time at constant optimized conditions. The refractive index n and extinction coefficient k of each monolayer were evaluated using ellipsometer (Elli-SE) in the visible range from 350 to 750 nm with a step with of 5 nm. The transmittance and reflectivity of the films were estimated using a UV-VIS-NIR spectrophotometer (KONICAMINOLTA CM-3600d). Measurement was performed at a 5 degree incident angle with a light source of D65. The Commission International de l'Eclairage (CIE), which is an international organization concerned with light and colour, has developed many numerical methods to quantify colour. The colour quantization was reported using the $L^*a^*b^*$ colour system.

Results and Discussion

Phase identification

Fig. 2 represents the XRD patterns obtained from SnO_2 (40-55 nm)/Ag (10 nm)/ SnO_2 (30 nm)/ SiO_2 (10 nm)/ Nb_2O_5 (10 nm) multi layer film with various top SnO_2 layer thicknesses. As can be seen in Fig. 2, all the as-deposited multi layer films appear to be amorphous regardless of SnO_2 thickness. There was a broad diffraction peak at 26° for all samples that is caused by the glass substrate. This can be explained that thin film with about 100 nm thick and processed at room temperature has a nanocrystalline phase formed during DC/RF sputtering process. Another interesting feature seen in the Fig. 2 is that Ag (111) peaks could be observed around 38.3° after deposition Ag on $\text{SnO}_2/\text{SiO}_2/\text{Nb}_2\text{O}_5$ multi layer film.

Optical properties

To extract an accurate analysis from EMP simulation, the refractive index n and extinction coefficient k are necessary. Fig. 3 represents the measured refractive index n and extinction coefficient k for SiO_2 , Nb_2O_5 ,

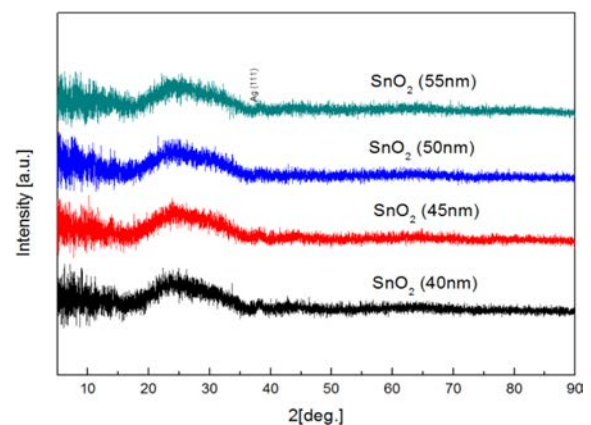


Fig. 2. XRD patterns obtained from the SnO_2 (40-55 nm)/Ag (10 nm)/ SnO_2 (30 nm)/ SiO_2 (10 nm)/ Nb_2O_5 (10 nm) multi layer film with various top SnO_2 layer thicknesses.

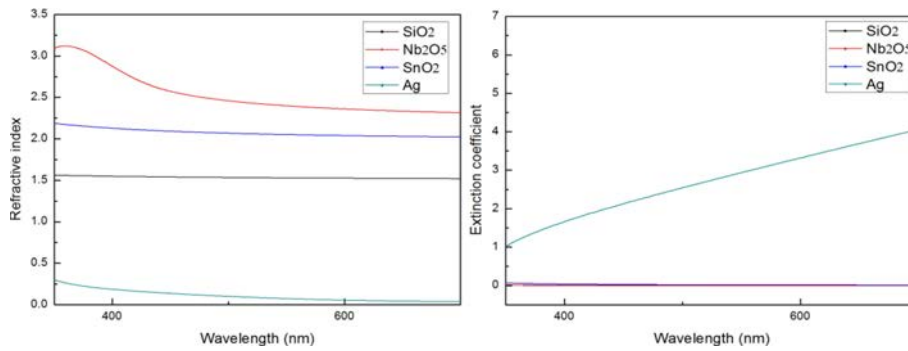
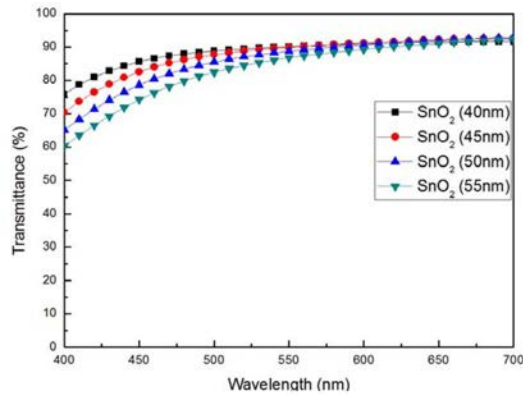
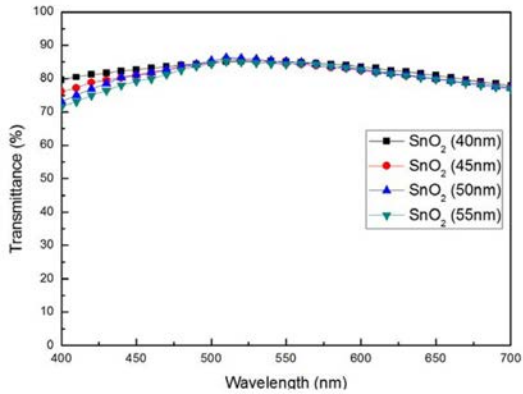


Fig. 3. The measured refractive index n and extinction coefficient k for SiO_2 , Nb_2O_5 , SnO_2 and Ag thin film in visible range, evaluated by ellipsometry measurement using ellipsometer.



(a)



(b)

Fig. 4. (a) Simulated and (b) experimentally measured optical transmittance spectra on the $\text{SnO}_2/\text{Ag}/\text{SnO}_2/\text{SiO}_2/\text{Nb}_2\text{O}_5$ multi layer films as a function of thickness of the top SnO_2 layer.

SnO_2 and Ag thin film in visible range, evaluated by ellipsometry measurement using ellipsometer (Elli-SE).

Prior to experiments, the optical programs named Essential Macleod Program (EMP) was carried out to simulate the optical characteristics. Based on results from a number of simulations, the film thickness of the top SnO_2 layer were varied from 40 to 55 nm, whereas the SiO_2 , Nb_2O_5 and Ag layers were fixed at 10 nm and the bottom SnO_2 layer was kept at 30 nm. Fig. 4(a) exhibited the optical simulation spectra of the transmittance on

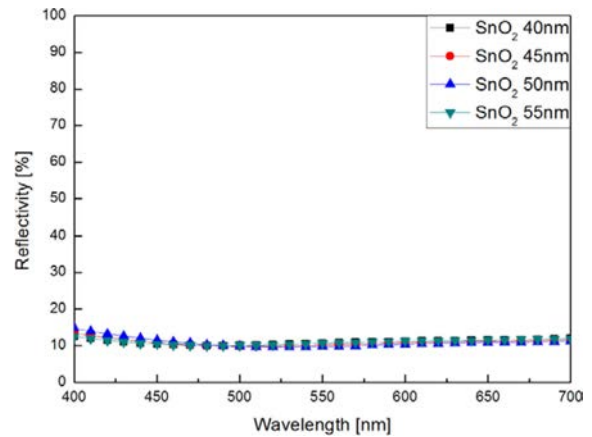


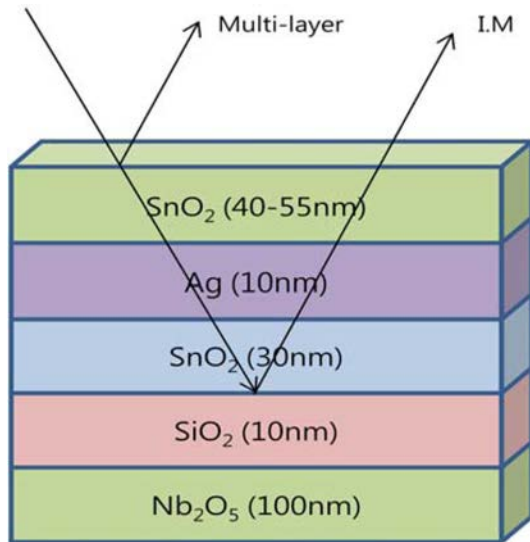
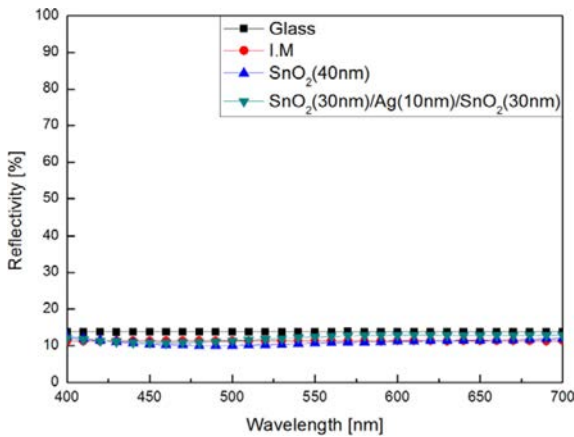
Fig. 5. The reflectivity-wavelength curves of $\text{SnO}_2/\text{Ag}/\text{SnO}_2/\text{SiO}_2/\text{Nb}_2\text{O}_5$ film with different top layer thickness of SnO_2 layer.

SnO_2 (40-55 nm)/ Ag (10 nm)/ SnO_2 (30 nm)/ SiO_2 (10 nm)/ Nb_2O_5 (10 nm) multi layer film as a function of the top layer of SnO_2 thickness. As can be seen from simulation spectra of Fig. 4(a), transmittance gradually decreased from 90.1 % to 86.7% at 550 nm wavelength with increasing the top SnO_2 thickness from 40 to 55 nm. Fig. 4(b) shows the experimentally measured transmittance taken from the same multilayer films as a function of the top SnO_2 thickness. As compared with that obtained through simulation, transparencies obtained from experimental spectra were slightly varied from 84.3 % to 85.1 % at 550 nm, and transmittance becomes gradually lowered. This might be attributed to light scattering on the each layer of film surface and interface instability due to elemental diffusion. Moreover, the deposition temperature was also considered to cause crystallinity difference of each layer between the experimental and EMP simulation results.

The reflectivity-wavelength curves of $\text{SnO}_2/\text{Ag}/\text{SnO}_2/\text{SiO}_2/\text{Nb}_2\text{O}_5$ film with different top layer thickness of SnO_2 are shown in Fig. 5 and the summarized results at 550 nm are displayed in Table I. As illustrated in Fig. 5, the reflectivity-wavelength spectra curves show a linear pattern and tend to constant regardless of wavelength change. Measured reflectivity was about 10% especially at 550 nm range, whereas the reference film of SnO_2

Table 1. Comparison of the reflectivity-wavelength curves of SnO₂/Ag/SnO₂/SiO₂/Nb₂O₅ film with different top layer thickness of SnO₂ at 550 nm.

Sample no.	Group	Reflectivity (%) at 550 nm
A	SnO ₂ (40 nm)/Ag(10 nm)/SnO ₂ (30 nm)/SiO ₂ (10 nm)/Nb ₂ O ₅ (10 nm)	10.6
B	SnO ₂ (45 nm)/Ag(10 nm)/SnO ₂ (30 nm)/SiO ₂ (10 nm)/Nb ₂ O ₅ (10 nm)	10.1
C	SnO ₂ (50 nm)/Ag(10 nm)/SnO ₂ (30 nm)/SiO ₂ (10 nm)/Nb ₂ O ₅ (10 nm)	9.7
D	SnO ₂ (55 nm)/Ag(10 nm)/SnO ₂ (30 nm)/SiO ₂ (10 nm)/Nb ₂ O ₅ (10 nm)	10.6
E	SnO ₂ (30 nm)/Ag(10 nm)/SnO ₂ (30 nm)	12.4

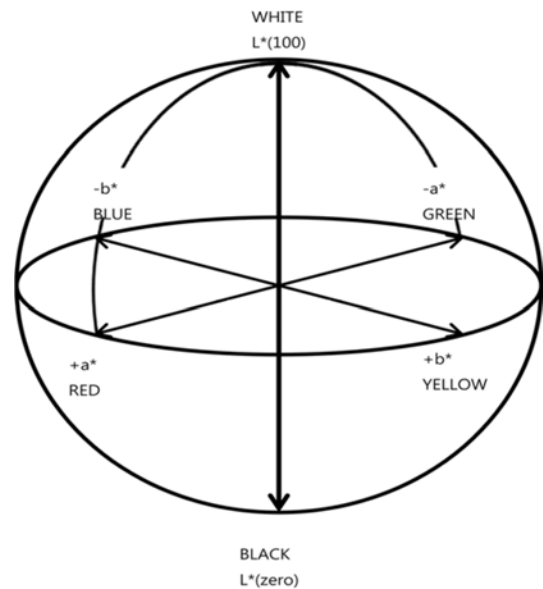
**Fig. 6.** Configuration of multi layer film to compare the reflectivities of two interfaces created by adjacent layers having mismatched refractive indices.**Fig. 7.** Reflectivities of curves in terms of different multi-layer film as a function of wavelength in visible range.

(30 nm)/Ag (10 nm)/SnO₂ (30 nm) shows 12.4%.

Fig. 6 illustrates a multi layer film configuration to compare the reflectivity of two interfaces created by adjacent layers having mismatched refractive indices. Particularly, reflectivities were compared with whole film surface that light can reflect off on the multi-layer film stackup and the interface only between IM layer and SnO₂, in which can give rise to the appearance of fringes due to a matrix of drive lines and sense line formed on

Table 2. The summarized results of reflectivities as a function of wavelength in visible range.

	450 nm (R ₁)	550 nm (R ₂)	650 nm (R ₃)
Glass	13.7%	13.8%	13.8%
I.M	11.3	11.3%	11.3%
A	10.4%	10.6%	10.8%
E	10.8%	12.4%	12.7%

**Fig. 8.** Schematic of the L*a*b* colour space.

TCO. Reflectivities as a function of wavelength were displayed in Fig. 7 and the results in visible range are shown in Table II. The reflectivities were measured on the different regions; a) substrate glass, b) interface between IM layer and SnO₂, c) the top surface of SnO₂ (40 nm)/Ag (10 nm)/SnO₂ (30 nm)/SiO₂ (10 nm)/Nb₂O₅ (10 nm) multilayer film and the reference film of SnO₂ (30 nm)/Ag (10 nm)/SnO₂ (30 nm), respectively.

As seen in Fig. 7, there was not much difference in reflectivities regardless of wavelength change. Especially at 450 nm and 550 nm in visible range, reflectivities of SnO₂ (40 nm)/Ag (10 nm)/SnO₂ (30 nm)/SiO₂ (10 nm)/Nb₂O₅ (10 nm) multi layer film, designated by sample A, were 10.4% and 10.6% measured on the top of multi-layer film stackup, whereas the reflectivities with IM layer only, designated by sample IM, were 10.8% and 12.4%, indicating that reflectivities variation was

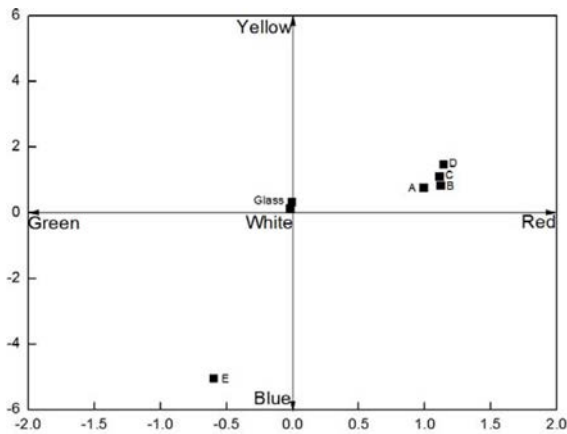


Fig. 9. The colour variation of different multi-layer films quantized by L*, a* and b*.

Table 3. The summarized data on different multi-layer films quantized in L*a*b* colour space.

Sample no.	L*	a*	b*
A	91.2	0.99	0.77
B	90.6	1.12	0.84
C	90.2	1.11	1.12
D	89.4	1.11	1.47
IM	95.4	-0.01	0.33
E	86.6	-0.6	-5.0

approximately within 2%.

Reflectivity spectra with different films can be represented in the CIE L*a*b* colour space [20]. The L*a*b* colour space indicates colour by accounting for both reflectivity spectra of material, which is the optical property of materials and the sensitivity to the visible spectra of human eye. Fig. 8 illustrated schematic of the L*a*b* colour space. The L*a*b* colour space describes colour appearance by dividing it into three coordinates; L*; a*; and b*. As the vertical axis, L* stands for lightness or brightness, its value run from zero through 50 at the center and reach 100 at the top of the sphere. The corresponding brightness varies from black at zero upward to pure white at 100. As horizontal axes, a* and b* are the chromaticity coordinates, and the signs and magnitude indicate hues and saturation, respectively. Plus and minus signs of a* are assigned for colour in red and green directions and those sign designation of b* are in yellow and blue direction. Fig. 9 demonstrates the colour variation of different multi-layer films quantized by L*, a*, and b*. Table III shows summarized data in L*a*b* colour space. As seen in Fig. 9, most of multi-layer films, except glass substrate, are locating almost at the same regions, dominantly bright yellow with a small contribution from red. Based on the L*a*b* colour space, it can be found that the lightness (+ L*) decreased from 91.2 to 89.4, whereas the yellowness (+ b*) increased from 0.77 to 1.47, with increasing SnO₂ top layer thickness

in multi-layer film. As compared the colours with sample A (SnO₂ (40 nm)/Ag (10 nm)/SnO₂ (30 nm)/SiO₂ (10 nm)/Nb₂O₅ (10 nm)) film and IM (SiO₂ (10 nm)/Nb₂O₅ (10 nm)) film, it is seen that colour of multi layer film with IM layer turns more brightness and less yellowish than sample A. Therefore it can be concluded that about 2% range of reflectivity and colour variation in the film with IM layer could be possibly used to reduce the visibility of drive lines and sense lines in touch sensor panel formed in TCO.

Conclusions

In summary, the characteristics of the RF/DC sputtering grown hybrid structure of SnO₂/Ag/SnO₂/SiO₂/Nb₂O₅ with varying the SnO₂ thicknesses and SnO₂/Ag/SnO₂ with IM layer were systematically investigated. In order to estimate the optical characteristics and compare them with experimental results, EMP was adopted and the refractive index *n* and extinction coefficient *k* were measured. The transmittances were dependent on the SnO₂ thickness. As compared with that obtained through simulation, transparencies obtained from experimental spectra were slightly varied from 85.1% to 84.3% at 550 nm, somewhat lower than simulated ones. The XRD patterns obtained from the SnO₂/Ag/SnO₂/SiO₂/Nb₂O₅ multi layer film appear to be amorphous. Based on reflectivity-wavelength spectra curve, reflectivities of SnO₂ (40 nm)/Ag (10 nm)/SnO₂ (30 nm)/SiO₂ (10 nm)/Nb₂O₅ (10 nm) multi layer film measured at 450 nm and 550 nm in visible range, were 10.4% and 10.6% on the top of multi-layer film stackup, respectively, whereas reflectivities with IM layer only were 10.8% and 12.4%, suggesting that reflectivity variation was approximately within 2%. From the L*a*b* colour space represented by reflectivity-wavelength spectra, it can be found that the lightness (+ L*) decreased from 91.2 to 89.4, whereas the yellowness (+ b*) increased from 0.77 to 1.47, with increasing SnO₂ top layer thickness in multi-layer film. As compared with multilayer film with 40 nm thickness of SnO₂ and IM layer, it was seen that colour of multi layer film with IM layer turns more brightness and less yellowish.

Acknowledgments

This work was supported by Industrial Technology Innovation Program funded by the Ministry of Trade, Industry and Energy (MOTIE, Korea) (No. 10040000-10048659).

References

- Podlogar M, Richardson JJ, Vengust D, Daneu N, Samadzija Z, Bernik S, Recnik, *Advanced Functional Materials*, 22 (2012) 3136-3145.

2. R. Lachaume, W. Favre, P. Scheiblin, X. Garros, N. Nguyen, J. coignus, D. Munoz, G. Reibold, *Energy Procedia*, 38 (2013) 770-776.
3. L. Liu, S. Mam, H. Wu, B. Zhu, H. Yang, J. Tang, X. Zhao, *Materials Letters*, 149 (2015) 43-46.
4. Q. Wan, E.N. Dattoli, W. Lu, *Applied Physics. Letters*, 90 (2007) 222107.
5. S. Yu, W. Zhang, L. Li, D. Xu, H. Dong, Y. Jin, *Thin Solid Films*, 552 (2013) 150-154.
6. H.J. Kim, K.W. Seo, Y.H. Kim, J.Y. Choi, H.K. Kim, *Applied Surface Science*, 328 (2014) 215-221.
7. D.R. Sahu, S.Y. Lin, J.L. Huang, *Applied Surface Science*, 252 (2006) 7509-7514.
8. A.E. Hajj, B. Lucas, M. Chakaroun, R. Antony, B. Ratier, M. Aldissi, *Thin Solid Films*, 520 (2012) 4666-4668.
9. D.R. Sahu, J.L. Huang, *Thin Solid Films*, 516 (2008) 4728-4832.
10. C.H. Hong, Y.J. Jo, H.A. Kim, J.H. lee, J.S. Kwak, *Thin Solid Films*, 519 (2011) 6829-6833.
11. X. He, W. Wang, S. Li, Y. Liu, W. Zheng, Q. Shi, X. Luo, *Vacuum*, 120 (2015) 17-21.
12. J.H. Kim, J.H. Lee, S.W. Kim, Y.Z. Yoo, T.Y. Seong, *Ceramic International*, 41 (2015) 7146-7150.
13. S.X. Zhang, S. Dhar, W. Yu, H. Xu, S.B. Ogale, T. Vendatesan, *Applied Physics Letters*, 91 (2007) 112113.
14. J.H. Kim, H.K. Lee, J.Y. Na, S.K. Kim, Y.Z. Yoo, T.Y. Seong, *Ceramic International*, 41 (2015) 8059-8063.
15. D. Miao, S. Jiang, S. Shang, Z. Chen, *Vacuum*, 106 (2014) 1-4.
16. D. Miao, S. Jiang, S. Shang, Z. Chen, *Ceramics International*, 40 (2014) 12847-12853.
17. A. Dhar, T.L. Alford, *Journal of Applied Physics*, 112 (2012) 103113.
18. C. Tung, E. Dorjgotov M. Kuwabara, S. Kang, C. Chen, J.Z. Zhong, *US Patent Application 20150316689 A1* (2015).
19. L. Huang, S.C. Chang, N. Oldham, S.P. Hotelling, J. Z. Zhong, C.H. Tung, *US Patent Application 20100141608 A1* (2010).
20. American Society for Testing Materials, *Symposium on Colour*, ASTM, Philadelphia, PA, 1941, p.3.